Low Dimensional Materials and Catalysts

MS.7.P205
Towards controllable growth of SiGe single and double quantum dot nanostructures

Y. Ma[1], S.F. Huang[1], C. Zeng[2], T. Zhou[1], Z. Zhong[1], Y.L. Fan[1], X.J. Yang[1], J.S. Xia[2], Z.M. Jiang[1]

[1]Fudan University, Physics, Shanghai, China
[2]Huazhong University of Science and Technology, School of Optoelectronic Science and Engineering, Wuhan, China

biglan001@gmail.com
Keywords: MBE, single quantum dot, double quantum dot

Fabrication of semiconductor single and double quantum dot (QD) nanostructures is of utmost importance due to their promising applications in the study of advanced cavity quantum electrodynamics [1], quantum optics [2] and solid-state spin qubits [3]. For those applications, one of the greatest challenges is the precise control of positions of the QDs. For applications based on single QDs (SQDs), fabrication of QDs with low areal density and at controllable sites is highly desirable. For the applications of double QDs (DQDs), a scalable self-assembled DQD system with precise control of dot spatial position, dot size and interdot spacing (the distance between the apexes of two dots in a DQD) is in demand. Morever, for a DQD system, by controlling the interdot spacing between two QDs, one can systematically study the coupling and coherence of electronic states in the two QDs that are strictly necessary for the creation of future functional units in quantum computing.

In this paper, we focused on the controllable growth of SiGe SQD and DQD nanostructures on nanhole-patterned Si substrates via molecular beam epitaxy (MBE). An ultra-low areal density down to $1x10^7$ cm^{-2} was achieved for both SQDs and DQDs with the corresponding periodicity as large as 3 μm. The SiGe DQD occupation in the nanoholes showed critical dependence on the Ge deposition amount. We also demonstrated that the interdot spacing between the two dots in a DQD could well be adjusted by varying the nanohole elongation ratio.

Figures 1(a) and (b) show the nanoholes with precisely controlled sizes and shape fabricated on the Si (001) surfaces via electron beam lithography (EBL) and reactive ion etching (RIE). The nanoholes are elongated along Si <110> with different length-width ratios (*r*).By optimizing the growth parameters, SQDs and DQDs were both realized on nanohole-patterned substrates with a periodicity down to 3 μm, as shown in figures 1 (c) and (d), respectively. Figures 2(a)-(d) show the three-dimensional (3D) morphology evolution of a DQD unit-cell at different Ge deposition amounts, 2.4, 3.0, 3.6 and 4.4 ML respectively. The AFM linescans crossing the DQD structures along Si <110> in figures 2(a)-(d) were shown in figure 2(e). It was found that only in a narrow Ge amount 'window' the DQD was formed. Neither too little or overdose Ge amount resulted in the formation of DQDs. Figures 3(a)-(c) show AFM images of a SiGe DQD grown on nanohole patterns with different elongation ratios of *r*. Figure 3(d) clearly shows that the interdot spacing monotonically increases with increasing *r*.

For nanoholes with a certain elongation ratio (e.g. *r*=3), whether a SQD or DQD formed at the nanoholes was found to be pre-determined by the Si buffer layer growth temperature, which was explained by different surface chemical potential distributions in the nanoholes after the buffer layer growth at different temperatures. Figures 4(a)-(c) show the surface morphologies of the nanoholes after growth of Si buffer layer at different temperatures. Figures 4(d)-(f) show the corresponding AFM images of the SiGe DQDs, which were grown by deposition 3.6 ML Ge at 450-550℃. It is found that low buffer layer growth temperature benefits the DQD formation. Figures 4(g)-(i) show the calculated surface chemical potential distributions for the nanoholes as shown in figures 4(a)-(c), respectively. The calculated results confirm that the SiGe QDs nucleate and grown at the sites of surface chemical potential minimum. Two minimum sites appear in the nanohole (figure 4(g)) for which the Si buffer layer is grown at the low temperature of 350℃ (figure 4(a)), which assures the growth of a DQD in a single nanohole.

1. V. Baumann, et al., Appl. Phys. Lett. 100, (2012), 091109.
2. Z. L. Yuan, et al., Science 295, (2002), 102.
3. B. M. Maune, et al., Nature 481, (2012), 344.

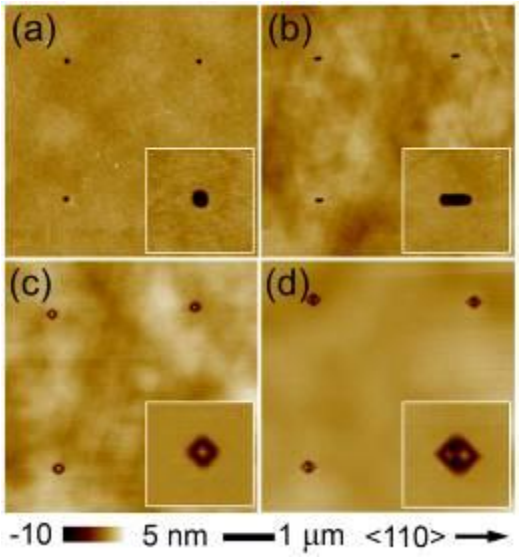

Figure 1. AFM micrographs of the nanohole pattern with a periodicity of 3 μm and different ratios of *r*. (a) *r*=1 and (b) *r*=3. Surface morphologies of the SiGe SQD (c) and DQD (b) grown on (a) and (b), respectively. Insets show enlarged AFM images of a single nanostructure.

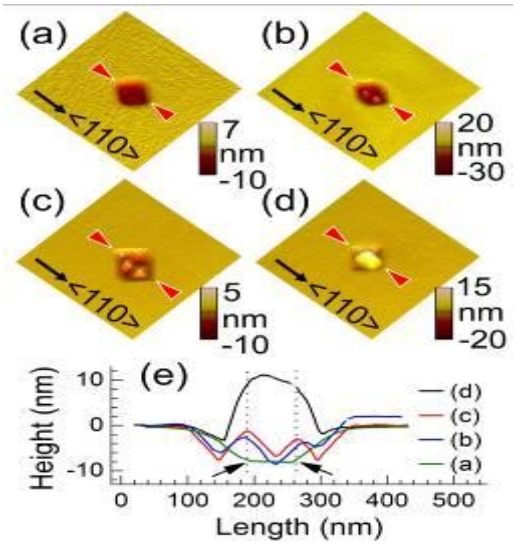

Figure 2. 3D AFM images of SiGe DQDs during the deposition of Ge (a) 2.4 ML, (b) 3.0 ML, (c) 3.6 ML and (d) 4.4 ML for nanoholes with r=3. The images are 800 x 800 nm2 in size. (e) The height profiles of the DQDs in corresponding evolution stages. The arrows and dash lines indicate the nucleation positions of the DQDs.

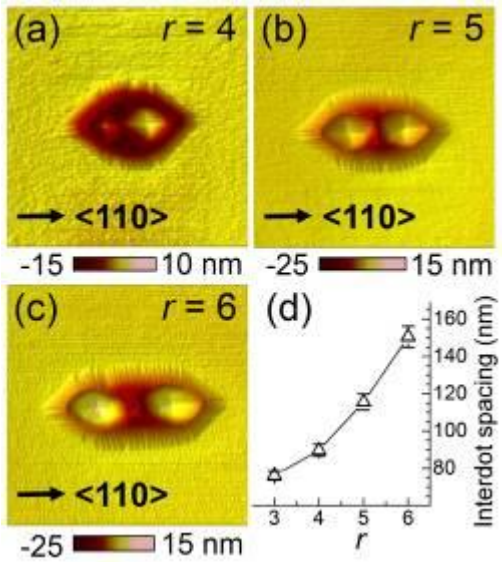

Figure 3. AFM micrographs of a single SiGe DQD unit-cell grown on nanohole patterns with different nanohole elongation ratios, (a) *r*=4, (b) *r*=5, (c) *r*=6. (d) The interdot spacing as a function of the elongation ratio. The images are 500 nm x500 nm in size.

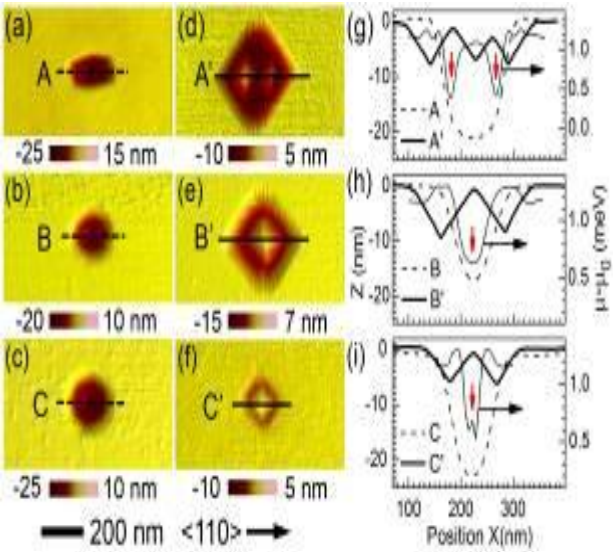

Figure 4. AFM micrographs of the nanoholes (*r*=3) after growth of a 45-nm-thick Si buffer layer at different temperatures, (a) 350℃, (b) 400-450℃, (c) 450℃, and the corresponding DQD growth results (d)-(f). (g)-(i) show the corresponding height profiles along the lines indicated in the AFM micrographs, along with the calculated surface chemical potential distributions in the nanoholes after the buffer layer growth.